

# Numerical analysis of a prestressed bridge considering construction processes.

Marcela P. Miranda<sup>1</sup>, Jorge P. Tamayo<sup>2</sup>, Inácio B. Morsch<sup>3</sup>

<sup>1,2,3</sup>*Dept. of Civil Engineering, Federal University of Rio Grande do Sul  
99, Osvaldo Aranha Avenue, Porto Alegre, 90035190, Rio Grande do Sul, Brazil  
<sup>1</sup>palhares.miranda@ufrgs.br, <sup>2</sup>jorge.tamayo@ufrgs.br, <sup>3</sup>morsch@ufrgs.br*

**Abstract.** Significant variations in geometry and supporting conditions can take place during the construction process of structures. These situations certainly influence the distributions of internal forces, displacements, and other structural responses during the construction phase and serviceability life of the structure, as customary occur in multi-span bridges. Thus, it is important to highlight these effects since collapses are recurrent during the construction period. In this sense, this study aims to contribute to a better understanding of structures during the construction phase by using numerical analysis. The sequential construction analysis is modeled using a ghost approach, which is coded into a three-dimensional finite element program, named VIMIS, developed at the PPGEC/UFRGS. To verify the code implementation in the context of the viscoelastic behavior of materials, a prestressed concrete bridge is analyzed, including the construction conditions, creep, shrinkage and relaxation effects. The obtained results expressed in terms of displacements and stresses are then compared with those of an academic software. As expected, VIMIS can capture the structural effects associated with construction phasing, reinforcing the necessity of include these analyses in structural designs.

**Keywords:** construction process, prestressed structures, ghost structures, numerical simulations.

## 1 Introduction

Over the last decades, the considerable development of materials, construction methods, and theoretical research have enabled the design and building of magnificent and challenging bridges. The design of these structures is increasingly complex, and engineers need to assess each phase of the entire process to ensure safety and performance. During the construction phase, the loading cases and changes in the geometric and support conditions are responsible for a complex variation of the stresses and deformations. According to recent works [1,2], the efforts from the construction phase may be the most important in bridge design, especially when considering the time effects. Unreliable and inappropriate analyzes of the construction stages might result in a partial or total collapse of the structure, even during the execution process, as occurred in the recent years [3,4].

As stated by Cruz (1995) [5], models to analyze and study structures during the construction phase need to present the possibility to include time effects analysis, such as creep, shrinkage, steel relaxation, second order effects, material nonlinearity, and generality regarding construction methods. Over the years, particular computational codes and commercial software have been developed and applied to the study of bridges during the construction process [1,2,6–9], but recent works have favored commercial finite element programs.

In [6], [7] and [9] the focus was on the importance of including the construction analysis in projects. Using SAP2000, Ates (2011) [6] studied a box concrete bridge considering the linear viscoelastic behavior of the materials and geometric nonlinearities. The results indicated a significant influence of the construction stage analysis in the internal forces, such as bending moments that were higher than those of the model without this analysis. The same software and material constitutive behavior were used by Adanur et al. (2012) [7] in the study of a suspension bridge. As already noted, relevant differences were observed with the model that

considered the construction staging of the structure.

In [9] the authors studied a prestressed box bridge constructed by the balanced cantilever method using MIDAS software. Linear constitutive relationships for materials and time effects were considered. Differences about 10% were observed between the analyses, with the model without stage analysis showing lower and not as expected stress values.

Another important issue involving the study of the execution phase is to investigate the influence of the construction sequential process on the structural behavior. In the case of cable-stayed bridges, the stays stressing procedures can affect the distribution of strains and the internal forces along the deck. Therefore specific construction analysis must be applied to define the best stays stress procedure [10,11]. Regarding concrete decks and steel-concrete composite decks, the pouring sequence of the slabs is important for the appearance of cracks. In addition, factors such as temperature gradient and curing days can further aggravate cracking [8,12,13]. Based on a construction stage analysis, performed with MIDAS software, He et al. (2020) [14] verified the advantages of a new pouring construction methodology that proved capable of reducing the compression stress at the top of the slab.

Given the aforementioned researches and the importance of considering the bridges construction period for reliable design results, in this paper, a prestressed concrete bridge is evaluated in a particular code, named VIMIS developed by the authors at the PPGEC/UFRGS, considering the execution process to verify the implementation of new routines related to the evaluation of the construction stages, employing the activation/deactivation approach [15].

## 2 Finite element model

The followings subtopics present brief details about the model considered in the study, including the constitutive models and the finite element formulation. For more information, the reader is referred to the papers [16,17].

### 2.1 Reinforced concrete

A linear behavior for the concrete material and a long-term constitutive model based on the stress-strain relationship of viscoelasticity were considered. It was applied the Boltzmann's superposition principle, which is represented by the Volterra's integral expressed in eq. (1). In this equation, the total concrete strain  $\varepsilon_t$  is separated into a mechanical strain  $\varepsilon_c$  or stress-dependent strain, and a nonmechanical one  $\varepsilon_0$ , representing concrete shrinkage. The term  $J(t, t')$  is the creep compliance function and represents the strain at the time  $t'$  caused for a unit stress applied at time  $t'$ , considering small stress increments.

$$\varepsilon_t = \varepsilon_c + \varepsilon_0 = \int_0^t J(t, t') d\sigma(t') + \varepsilon_0 \quad (1)$$

The creep strain  $\varepsilon_{cc}$  can be isolated and expressed by the creep function  $C(t, t')$  which is usually obtained by approximation through Dirichlet series, as stated by eq. (2) and considering  $C(t, t') = J(t, t') - 1/E_c(t')$ . In this approach, a Generalized Kelvin model is used following eq. (3), in which the  $E_\alpha$  is the age-dependent modulus and  $\tau_\alpha$  is the retardation time of the term of the spring-dashpot system. At each loading time  $t'$ , a least square procedure is applied to obtain the age-dependent set of parameters (N).

$$\varepsilon_{cc} = \int_0^t C(t, t') d\sigma(t') \quad (2)$$

$$C(t, t') = \sum_{\alpha=1}^N \frac{1}{E_\alpha(t')} \left( 1 - e^{-(t-t')/\tau_\alpha} \right) \quad (3)$$

Considering different time instants, the procedure is to substitute eq. (3) into eq. (2) for each time step, integrate analytically, and obtain the creep incremental strain  $\Delta\varepsilon_{cc}$ . Considering the generic time interval  $\Delta t_i = t_{i+1} - t_i$ , the expression of the increment  $\Delta\varepsilon_{cc}(t_i)$  is written as showed in eq. (4) and eq. (5). In these equations, a linear

approximation is used to approximate the stress variation within a time interval by setting  $\xi = 1/2$ .

$$\Delta \varepsilon_{cc}(t_i) = \sum_{\alpha=1}^N \varepsilon_{\alpha}^*(t_{i-1}) \left[ 1 - e^{-(\Delta t_i)/\tau_{\alpha}} \right] + \sum_{\alpha=1}^N \frac{1}{E_{\alpha}(t_i - \xi)} \left[ 1 - \frac{\tau_{\alpha}}{\Delta t_i} \left( 1 - e^{-(\Delta t_i)/\tau_{\alpha}} \right) \right] \Delta \sigma(t_i) \quad (4a)$$

$$\varepsilon_{\alpha}^*(t_{i-1}) = \varepsilon_{\alpha}^*(t_{i-2}) e^{-(\Delta t_{i-1})/\tau_{\alpha}} + \left[ \frac{1 - e^{-(\Delta t_{i-1})/\tau_{\alpha}}}{E_{\alpha}(t_{i-1} - \xi)} \right] \frac{\tau_{\alpha}}{\Delta t_{i-1}} \Delta \sigma(t_{i-1}) \quad (4b)$$

The eq. (5) expresses a quasi-elastic stress-strain relationship in which  $E^*$  and  $\Delta \varepsilon^*$  are the equivalent material modulus and incremental strain, respectively, and the incremental stress is given by  $\Delta \sigma = \Delta \sigma(t_i) = \sigma(t_i) - \sigma(t_{i-1})$ .

$$\Delta \sigma = E^* (\Delta \varepsilon - \Delta \varepsilon^*) \quad (5)$$

where,

$$\Delta \varepsilon^* = \Delta \varepsilon_{sh} + \sum_{\alpha=1}^N \left[ \mathbf{D}_{\alpha}^{-1} \Delta \sigma_{i-1} + \varepsilon_{i-2} (e^{\Delta y_{\alpha,i-1}}) \right] \left[ 1 - e^{\Delta y_{\alpha,i}} \right] \quad (6a)$$

$$\frac{1}{E^*} = \frac{1}{E(t_i)} + \sum_{\alpha=1}^N \frac{1 - \Delta y_{\alpha}}{\left[ 1 - e^{\Delta y_{\alpha}} \right] E_{\alpha}(t_i - \xi)} \quad (6b)$$

In the eq. (6) the mentioned terms are explicit for the tridimensional case, written for a time step  $\Delta t_i = t_i - t_{i-1}$ , in which  $\Delta y_{\alpha} = \Delta t_i / \tau_{\alpha}$ ,  $\mathbf{D}_{\alpha}^{-1}$  is the viscoelastic constitutive matrix evaluated with an elasticity modulus equal to  $(1 - e^{\Delta y_{\alpha,i-1}}) / \Delta y_{\alpha,i-1}$ , with  $\Delta y_{\alpha,i-1} = \Delta t_{i-1} / \tau_{\alpha}$ .

## 2.2 Tendon

Tendons were analyzed considering the linear elastic behavior of the material resorting to a uniaxial stress-strain relationship. About the time effects, a prestressed loss increment  $\Delta \sigma_{pt,r}$ , due to steel relaxation, is calculated through eq. (7), based on the steel yield strength  $f_{py}$ , type of tendon relaxation  $k$ , and time interval  $t$  measured in hours from the instant in which the initial prestress  $\sigma_{po}$  is applied.

$$\Delta \sigma_{pt,r} = -\frac{\sigma_{po}}{k} + \left[ \log(t) \left( \frac{\sigma_{po}}{f_{py}} - 0.55 \right) \right] \quad (7)$$

## 2.3 Finite element

Figure (1) illustrates an eight-node thick shell element used to model the reinforced concrete. Each node has five degrees of freedom (three translations and two in-plane rotations). Several layers compose the element throughout the thickness from which the nonlinear behavior of the material can be reproduced. The steel reinforcement is represented by means of layers with equivalent thickness. On the other hand, the prestressed tendons are modeled with a one-dimensional element, composed of three nodes, and embedded within the shell element.

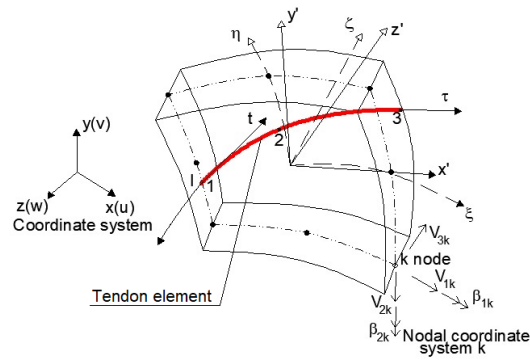


Figure 1. Shell finite element, curved tendon, and associated degrees of freedom.

### 3 Construction stage analysis of a prestressed concrete bridge

#### 3.1 Model

The construction process of a three-span symmetrical bridge was simulated using the activation/deactivation method in which the whole structure is modeled at once but using approximately null stiffness values for all elements at the start of the analysis, e.g.,  $1E-15$ . Thereafter, these elements are subsequently activated, with their real material properties, according to the construction phases. The bridge presents a box section and 172 m in length, as shown in Fig. (2). The cross section of the bridge is constant along the entire length of the structure with straight tendons. It is important to note that a simplification of the section was considered, since in the reference work [18] the cross section is varied and curved tendons were applied. All materials properties were the same. The construction sequence is described in Fig. (3) and Tab. (1).

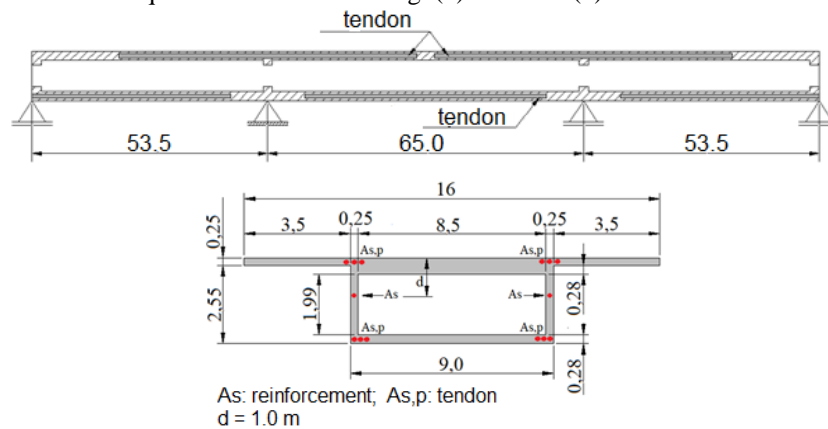


Figure 2. Dimensions of the bridge (unit: meters).

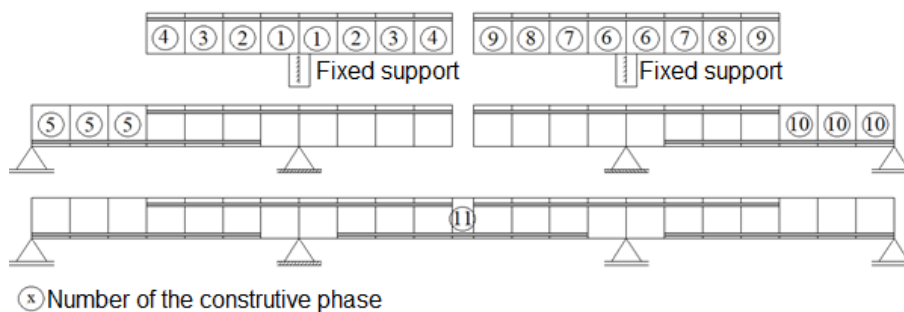


Figure 3. Construction sequence.

The precast segments were cured for 3 days and stored until the beginning of the execution. The analysis considered as loads the self-weight of the structure and a prestressing stress of 126 kN/cm<sup>2</sup> (1260 MPa). Concerning time effects, ACI[19] model was considered with type of cement III, relative moisture of 40%, and creep and shrinkage ultimate coefficients of 2.0 and 300x10<sup>-6</sup>, respectively. The prestressed steel was featured as low relaxation; therefore, the  $k$  parameter of the eq. (7) is equal to 45. Material properties can be verified in Tab. (2). It is important to emphasize that the results obtained with the present work were compared to that presented by an academic finite element model with beam elements, using the same material properties. Therefore, the Poisson's ratio is not considered and admitted as null. There is no other information about this property for this structure, so a null Poisson's ratio was adopted.

Table 1. Details of the construction phases.

Start of the stage (days)*	Stage	Activities
30	1	
33	2	
36	3	Assembly of the segments and activation of prestressing.
39	4	
43	5	Assembly of the segments, activation of prestressing, and change supports.
47	6	
50	7	
53	8	Assembly of the segments and activation of prestressing
56	9	
60	10	Assembly of the segments, activation of prestressing, and change supports.
63	11	Assembly of the central segment, activation of prestressing, and change supports.

\*Considering the age of the concrete

Table 2. Materials properties.

Material	Properties	
Concrete	Elastic modulus	3500 kN/cm <sup>2</sup>
	Poisson's ratio	0
	Compression strength	5.4 kN/cm <sup>2</sup>
Reinforcement	Elastic modulus	20000 kN/cm <sup>2</sup>
	Yield stress	58.5 kN/cm <sup>2</sup>
	Total area	222 cm <sup>2</sup>
Tendon	Elastic modulus	19000 kN/cm <sup>2</sup>
	Yield stress	150 kN/cm <sup>2</sup>
	Area (sup. <sup>1</sup> )	126 cm <sup>2</sup>
	Eccentricity* (sup. <sup>1</sup> )	120 cm
	Area (inf. <sup>2</sup> )	81.5 cm <sup>2</sup>
	Eccentricity* (inf. <sup>2</sup> )	125 cm

\*Considering the centroid <sup>1</sup>upper tendon <sup>2</sup>bottom tendon

In the VIMIS program, the finite element (FE) model is developed considering the middle plane of the structures and thickness discretization in layers, as aforementioned. To simulate a box section was necessary to use the parameter  $\beta$  for which a zero value is attributed to indicate non-existent layers, conversely a value of 1 means that the layer is present in the cross section. In this case, a rectangular cross-section was modeled, and null layers were assigned correspondingly to approximate the real section, as shown in Fig.(4a). The FE mesh of the structure is shown in Fig.(4b).

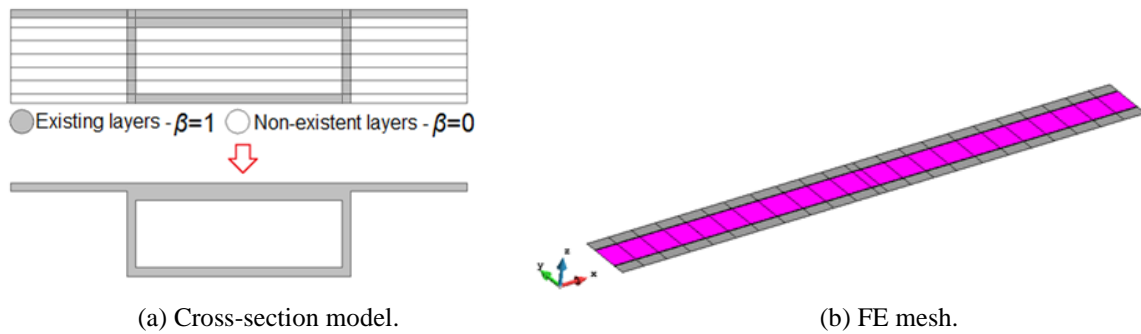


Figure 4. Finite element model.

### 3.2 Results

With the main objective of verifying the results obtained with VIMIS, a beam finite element model of the same structure was analyzed with an academic program available in [20] and developed for construction stage analysis of bridges. This program was applied in the cited reference to simulate the construction process of the original structure presented in [18], but using straight prestressed cables, and for which satisfactory results were obtained. Displacements and stress at the top and bottom of the cross-section were evaluated and compared, as shown in Fig. (5) and Fig (6).

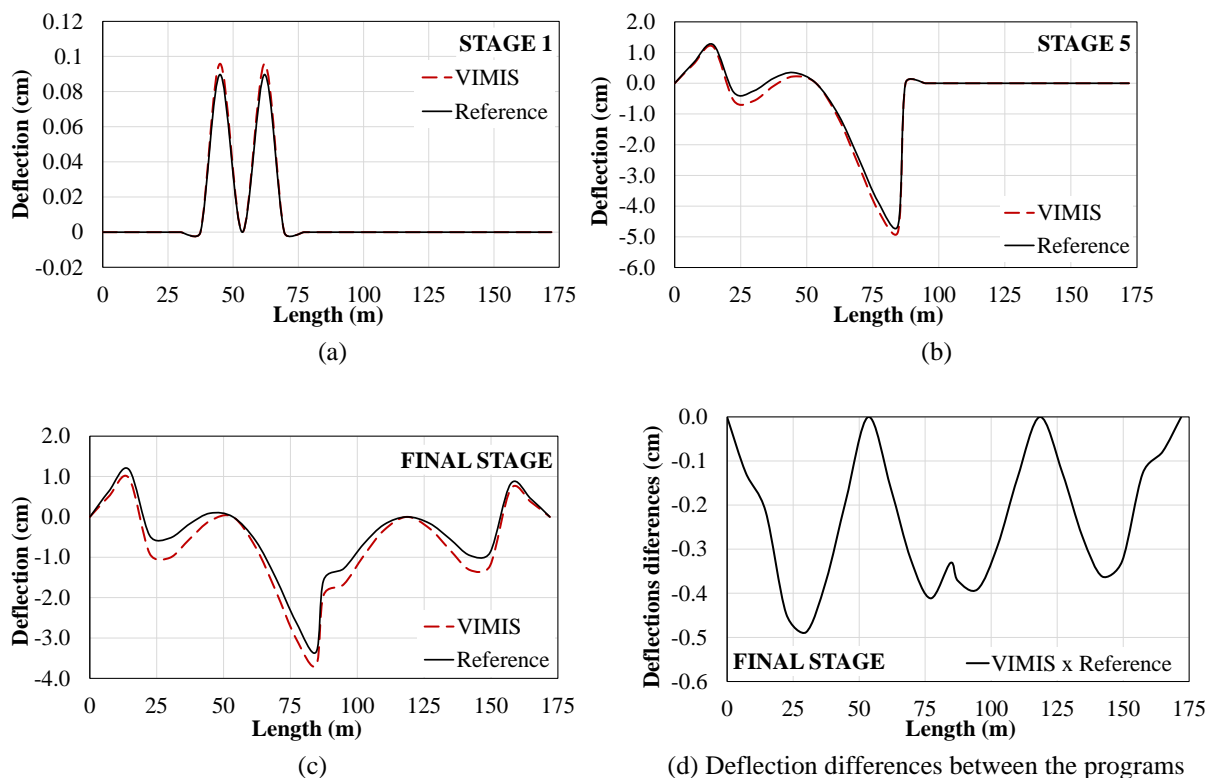


Figure 5. Vertical displacement results in some stages.

The Fig. 5 shows the optimal fit of present results with those of the reference in terms of deflections along the beam axis for various construction stages. As can be seen in Fig.(5d), the largest difference observed of vertical displacements is 5 mm and occurred in the side span of 53.5 m, which can be considered acceptable for practical processes. It should be noted that both viscoelastic models are not completely identical in the computational programs in the sense that the adjustment of the age-dependent parameters are different, and this aspect may

explain the observed differences. The stress results, present in Fig.(6), corroborate the above remarks and indicate the proper functioning of the section adjustment to a box section.

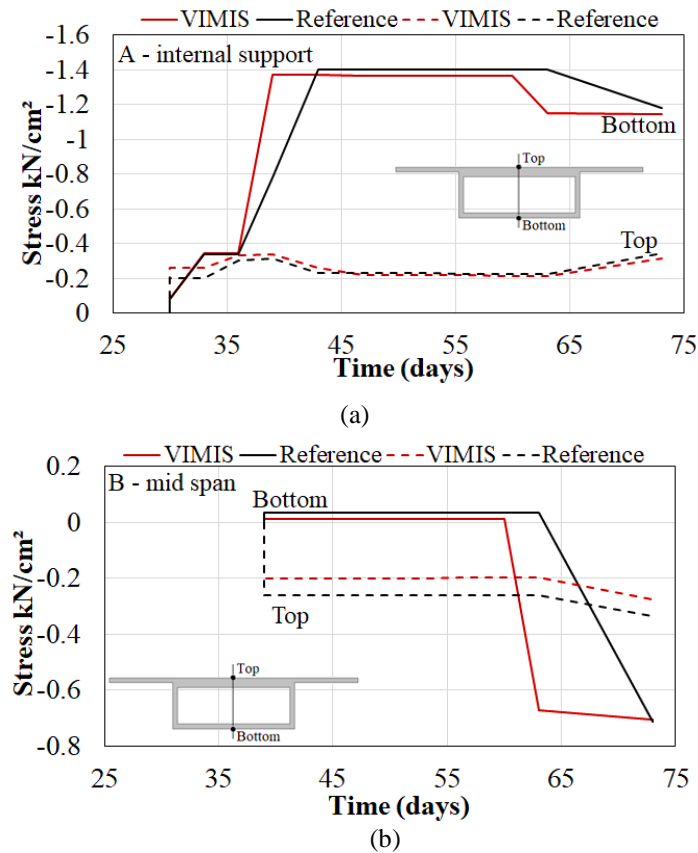


Figure 6. Variation of the stress throughout the stages.

## 4 Conclusions

The complexity of bridge systems reinforces the importance of developing designs that are better suited to the reality of the construction stages and the behavior of the structure in service. The construction process needs to be included in the analysis and study phase, considering all aspects arising from this stage. The results of this paper indicate the adequate working of the routines included in VIMIS to verify the execution process and show the potentiality of the program as a good tool to analyze structures with high complexity involving also long-term effects.

**Acknowledgements.** The authors gratefully appreciate the support provided by the Brazilian Research Council (CAPES) and the Federal University of Rio Grande do Sul (UFRGS).

**Authorship statement.** The authors hereby confirm that they are the sole liable persons responsible for the authorship of this work, and that all material that has been herein included as part of the present paper is either the property (and authorship) of the authors or has the permission of the owners to be included here.

## References

- [1] C. Han, J. Zhang, D. Zhou, S. Lan, P. Wang, Computing Creep Secondary Internal Forces in Continuous Steel–Concrete Composite Beam Constructed through Segmented Pouring., *J. Struct. Eng.* 146 (2020) 1-13p. doi:10.1061/(ASCE)ST.1943-541X.0002494.

- [2] G.-M. Wang, L. Zhu, G.-P. Zhou, B. Han, W.-Y. Ji, Experimental Research of the Time-Dependent Effects of Steel-Concrete Composite Girder Bridges during Construction and Operation Periods, *Materials* (Basel). 13 (2020) 1-18p. doi:10.3390/ma13092123.
- [3] M. Ayub, Investigation of March 15, 2018 Pedestrian Bridge collapse at Florida International University, Miami, FL., Washington, D.C., 2019.
- [4] Chijara Bridge Corficolombiana - Relevant Information., Corp. Financ. Colomb. (2018). <https://www.corficolombiana.com/wps/wcm/connect/corficolombiana/387181b2-30f4-4da4-b106-8462807dfa80/Informacion-relevante-30042018.pdf?MOD=AJPERES> (accessed February 21, 2019).
- [5] P.J.S. Cruz, Um novo modelo para análise não linear e diferida de estruturas evolutivas. Parte I: descrição geral., (1995) 5-16.
- [6] S. Ates, Numerical modelling of continuous concrete box girder bridges considering construction stages., *Appl. Math. Model.* 35 (2011) 3809-3820. doi:<https://doi.org/10.1016/j.apm.2011.02.016>.
- [7] S. Adanur, M. Gunaydin, A.C. altunisik, B. Sevim, Construction stage analysis of Humber Suspension Bridge., *Appl. Math. Model.* 36 (2012) 5492-5505p. doi:10.1016/j.apm.2012.01.011.
- [8] L.J. Butler, W. Lin, J. Xu, N. Gibbons, M.E.B. Elshafie, C.R. Middleton, Monitoring, modeling, and assessment of a self-sensing railway bridge during construction., *J. Bridg. Eng.* 23 (2018) 04018076. doi:10.1061/(ASCE)BE.1943-5592.0001288.
- [9] S.S.R. Vookunnaya, T. Thite, Construction Stage Analysis of Segmental Cantilever Bridge., *Int. J. Civ. Eng. Technol.* 8 (2017) 373-382p.
- [10] M. Arici, M.F. Granata, A. Recupero, The influence of time-dependent phenomena in segmental construction of concrete cable-stayed bridges., *Bridg. Struct.* 7 (2011) 125-137. doi:<https://doi.org/10.3233/BRS-2011-030>.
- [11] M. Granata, P. Margiotta, M. Arici, A. Recupero, Construction stages of cable-stayed bridges with composite deck., *Bridg. Struct.* 8 (2012) 93-106. doi:10.3233/BRS-120044.
- [12] L. Dezi, F. Gara, G. Leoni, Construction sequence modelling of continuous steel-concrete composite bridges decks., *Steel Compos. Struct.* 6 (2006) 123-128pp. doi:<https://doi.org/10.12989/scs.2006.6.2.123>.
- [13] L. Dezi, F. Gara, G. Leoni, Simplified method to analyse casting sequences of composite bridge slabs., *IABSE Symp. Rep.* 101 (2013). doi:10.2749/222137813808627325.
- [14] J. He, X. Li, C. Li, J.A.F.O. Correia, H. Xin, M. Zhou, A novel asynchronous-pouring-construction technology for prestressed concrete box girder bridges with corrugated steel webs., *Structures.* 27 (2020) 1940-1950. doi:10.1016/j.istruc.2020.07.077.
- [15] E.A. Hanafy, J.J. Emery, Advancing face simulation of tunnel excavation and lining placement., in: *Proc. 13th Can. Rock Mech. Undergr. Rock Eng.*, 1980: pp. 119-125.
- [16] B.D.S. Sánchez, J.P. Tamayo, I.B. Morsch, M.P. Miranda, A nonlinear geometric model for pre-stressed steel-concrete composite beams., *J. Brazilian Soc. Mech. Sci. Eng.* 43 (2021) 233. doi:10.1007/s40430-021-02938-1.
- [17] J.L.P. Tamayo, M.I. Franco, I.B. Morsch, J.M. Désir, A.M.M. Wayar, Some aspects of numerical modeling of steel-concrete composite beams with prestressed tendons., *Lat. Am. J. Solids Struct.* 16 (2019). doi:10.1590/1679-78255599.
- [18] M.K. Tadros, A. Ghali, W.H. Dilger, Long-term stresses and deformation of segmental bridges., *Precast. Concr. Institute. PCI-Journal.* 24 (1979) 66-87.
- [19] ACI-Committee-209, Guide for modeling and calculation shrinkage and creep in hardened concrete., American Concrete Institute, 2008.
- [20] K.W. Shushkewich, Analysis of segmental bridges, Universidade de Alberta, 1985.